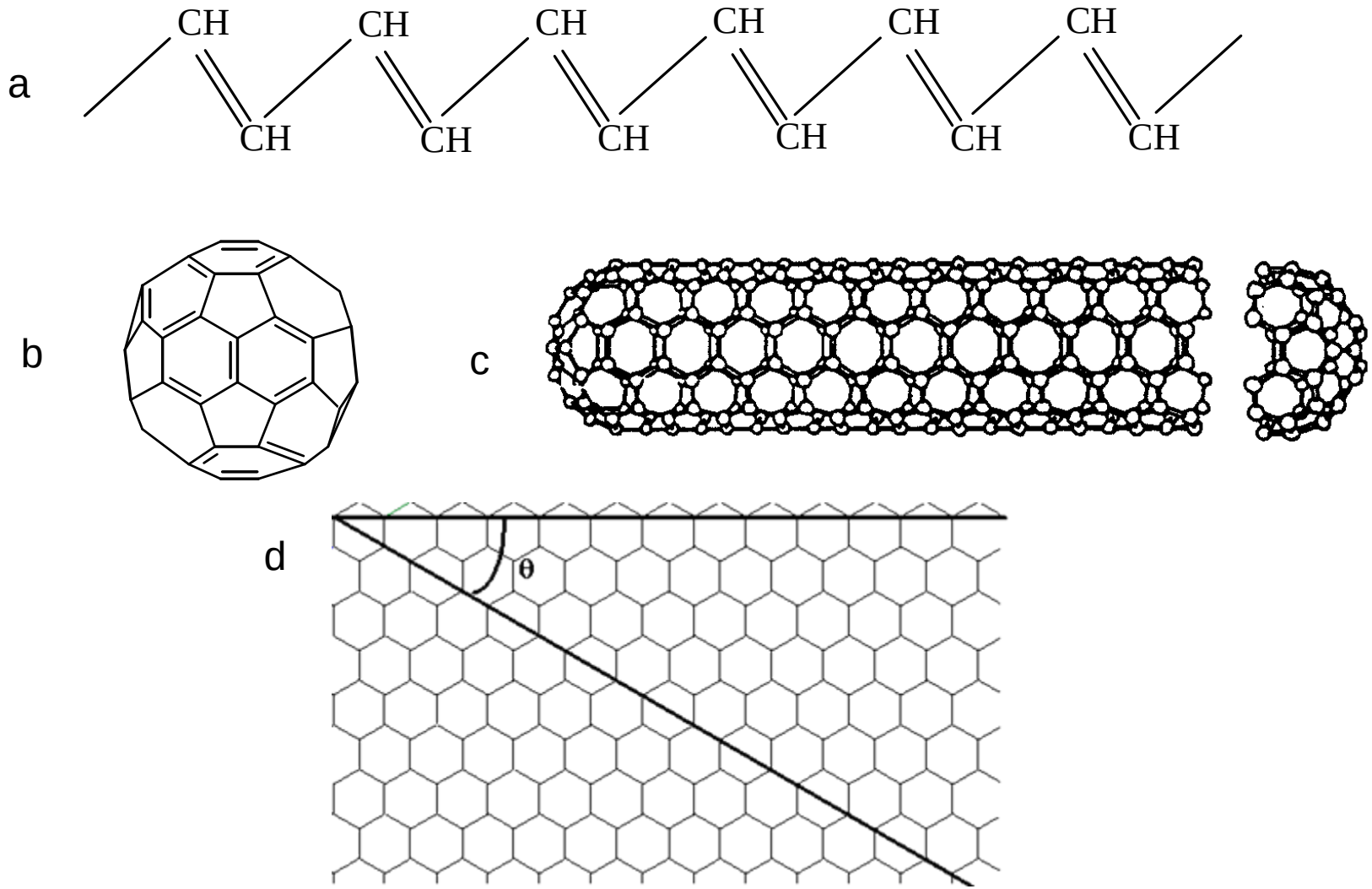

Figure 8. 1 Conjugated structures with different dimensionalities: (a) polyacetylene; (b) buckminsterfullerene C60; (c) [5,5] armchair SWNT; (d) schematically illustrating how the graphene sheet is rolled into a nanotube cylinder.

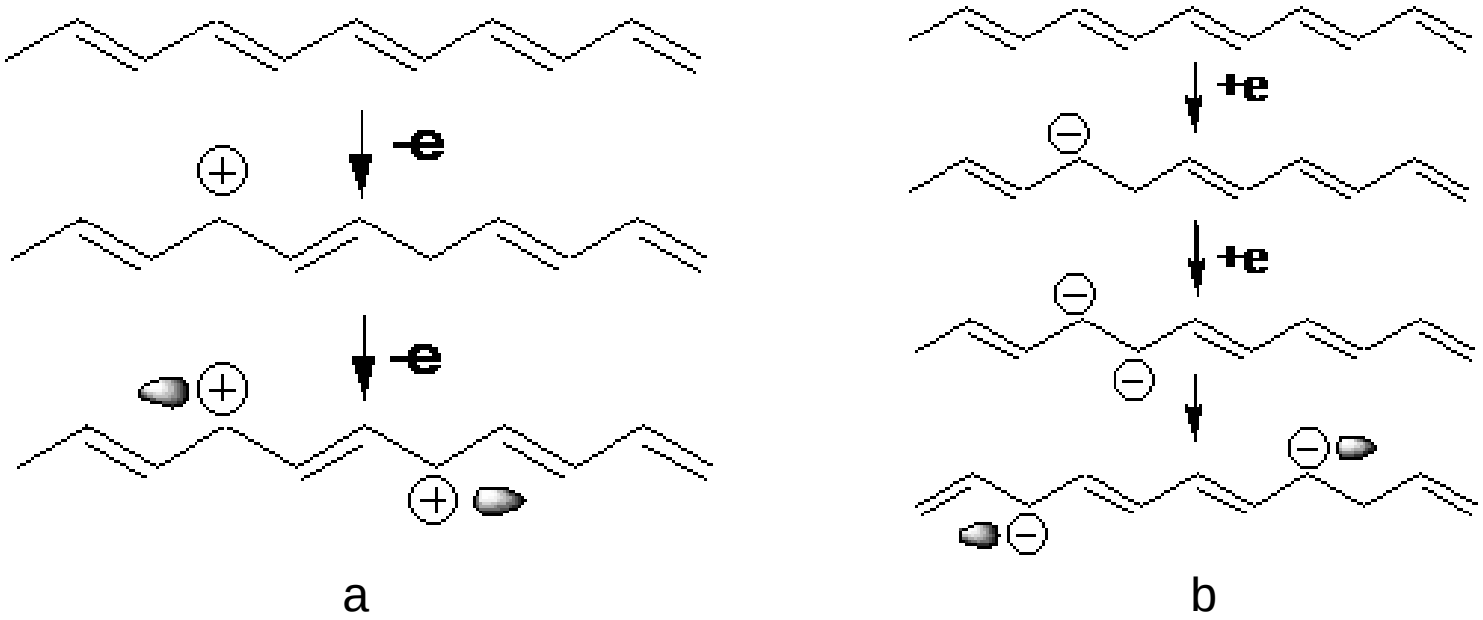

Figure 8. 2 A schematic description of the doping of *trans*-polyacetylene chain: (a) *p*-doping and (b) *n*-doping.

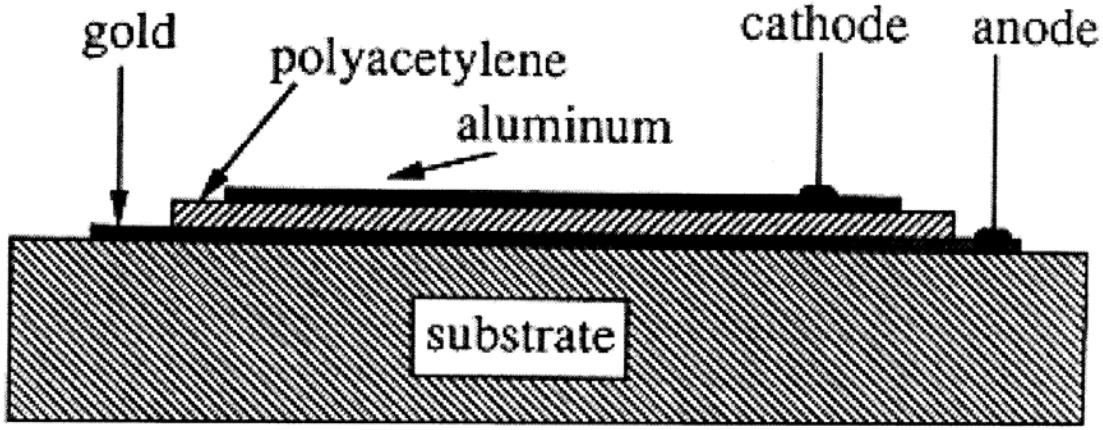

Figure 8. 3 A typical Schottky-barrier diode structure with a layer of polyacetylene (500-1000 nm) sandwiched between a thin layer of aluminum, chromium or indium (20 nm) and gold (20 nm) supported by a flat glass substrate.

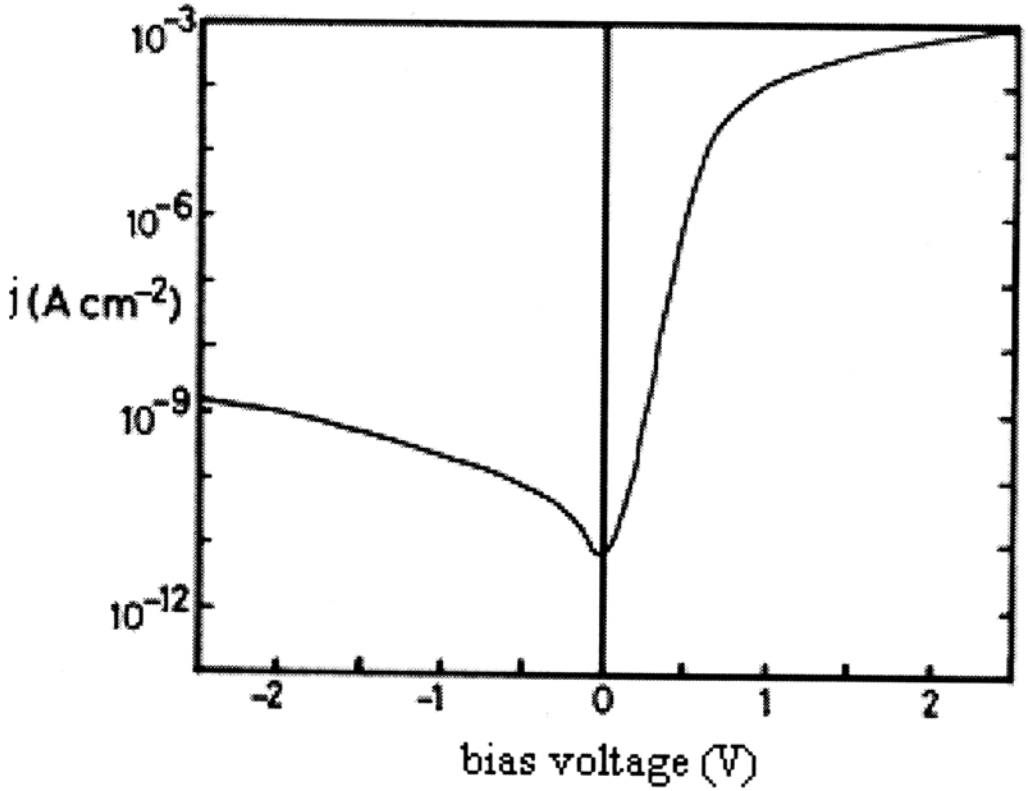

Figure 8. **4** Forward and reverse characteristics for a Schottky diode with the Al/polyacetylene/Au structure, which gives a very good diode characteristic with a forward to reverse ratio as high as 5 $\times$ 10^{10} at a bias of + 1.5 V.

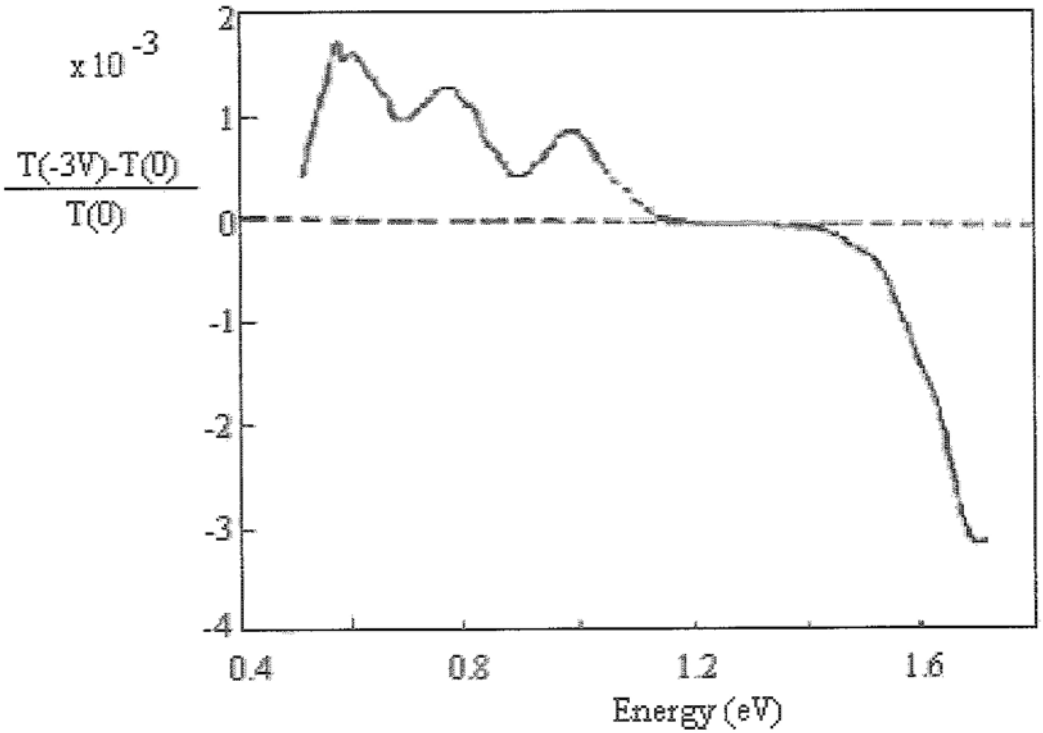

Figure 8. 5 Bias voltage modulated optical transmission for an Al/polyacetylene Schottky diode of thickness 900 nm. $T(V)$ is the optical transmission at bias voltage V.

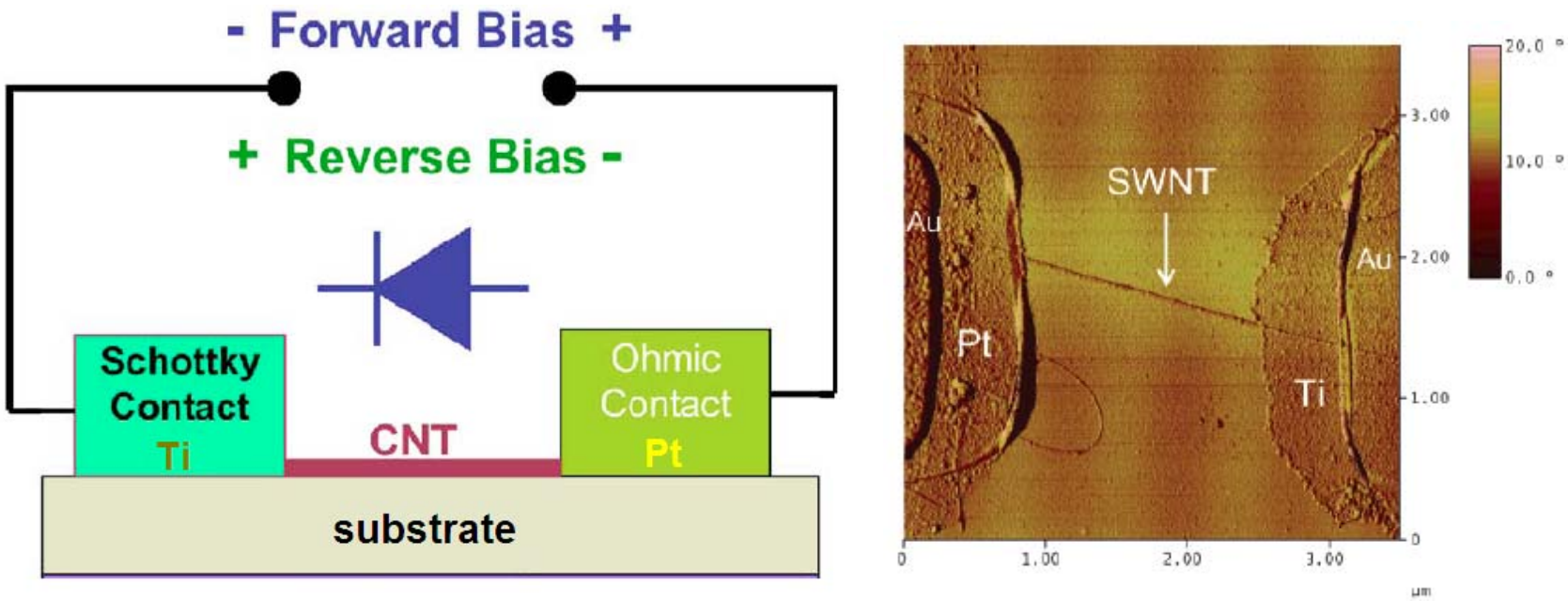

a b

Figure 8. 6 (a) Schematic representation of the SWNT-Schottky diode with Ti and Pt contacts, (b) a typical AFM phase plot image of the SWNT-Schottky diode.

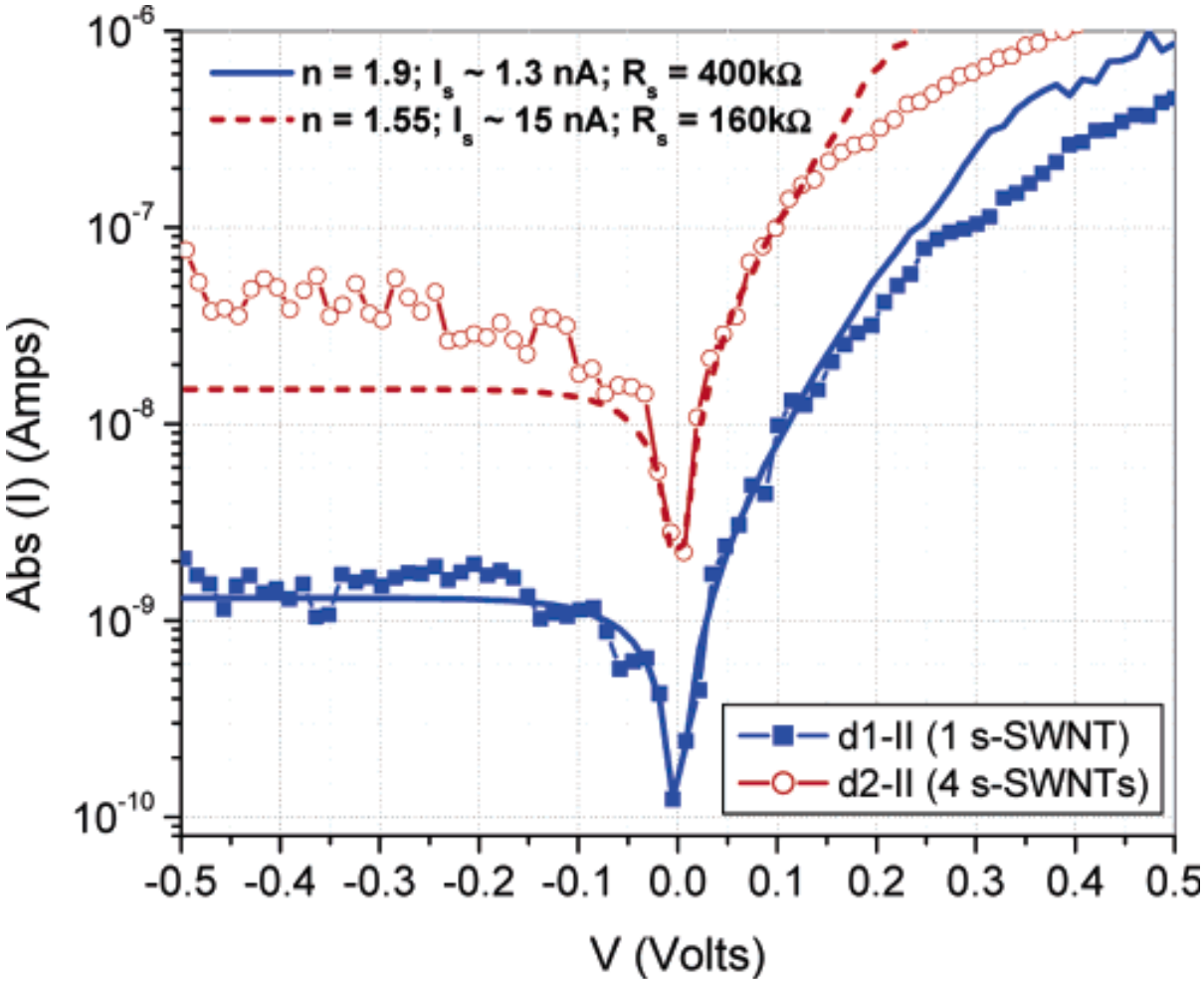

Figure 8. 7 Ideality curve fits in low bias range for d1-II (with single s-SWNT) and d2-II (with four s-SWNTs) Schottky diodes. The curve shows the absolute magnitude of the current plotted against the corresponding voltage.

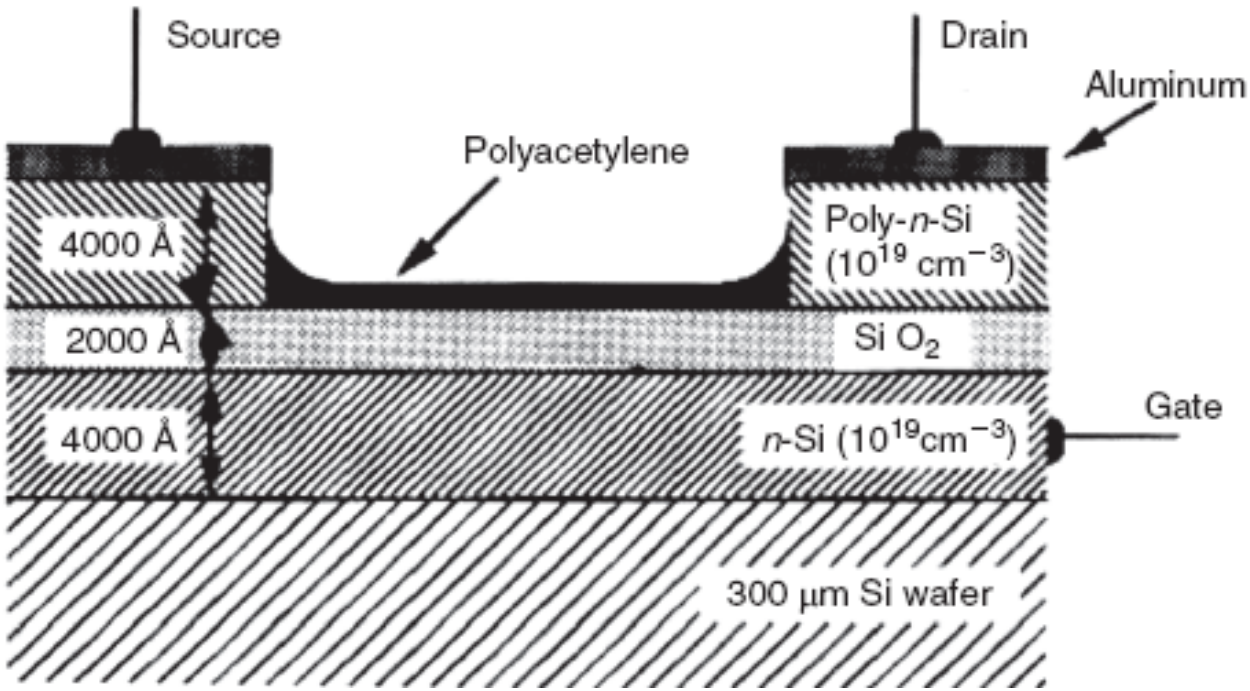

Figure 8. 8 A MISFET device fabricated on a silicon wafer substrate, using polyacetylene as the semiconductor, silicon dioxide as the insulator layer, heavily *n*-doped silicon as the bottom metallic layer (the gate), the source and drain contacts. Aluminum is used as a blocking contact.

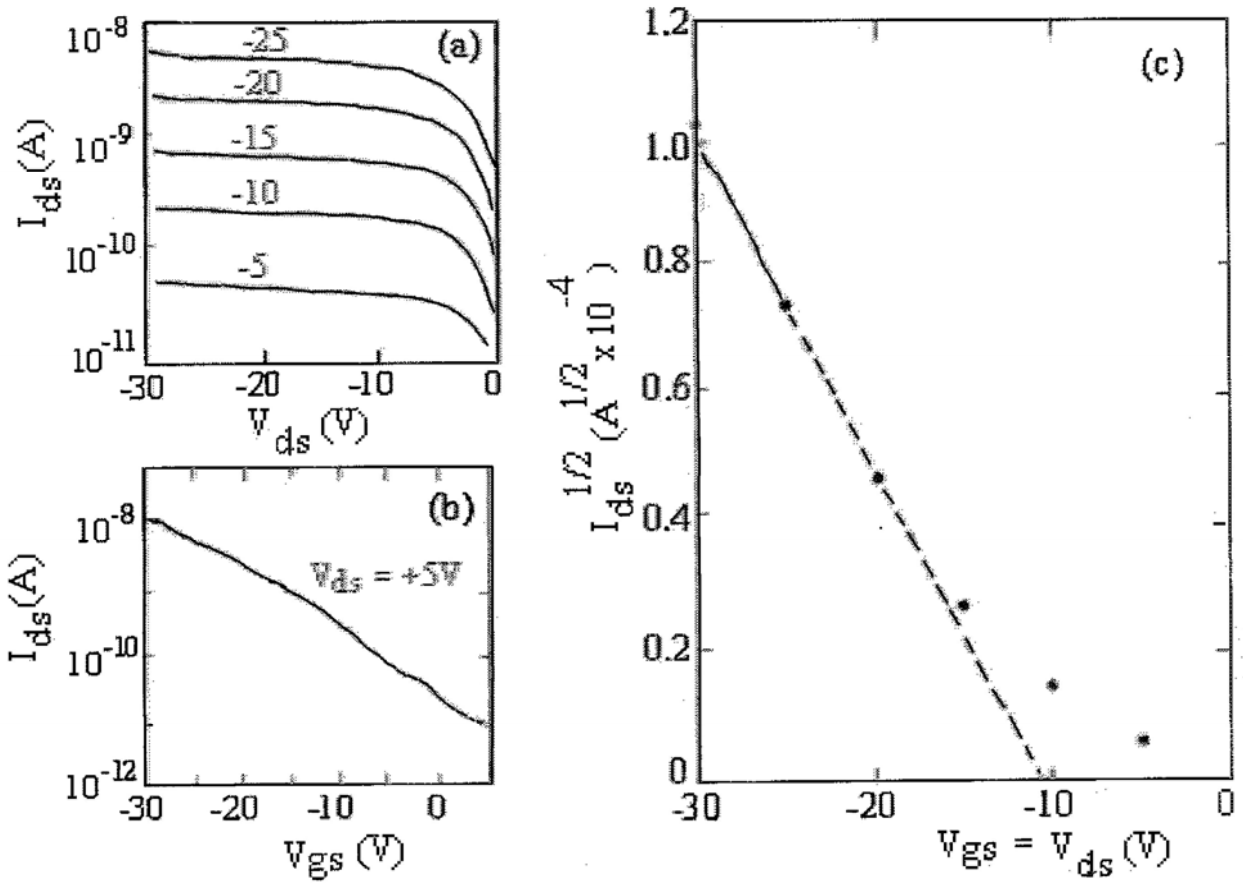

Figure 8. **9** Characteristics of MISFET transistor with Au source and drain contacts. (a) I_{ds} versus V_{ds} for various negative values of V_{gs}; (b) I_{ds} versus V_{gs} for V_{ds} = + 5 V; (c) $(I_{ds})^{1/2}$ versus $V_{ds} = V_{gs}$.

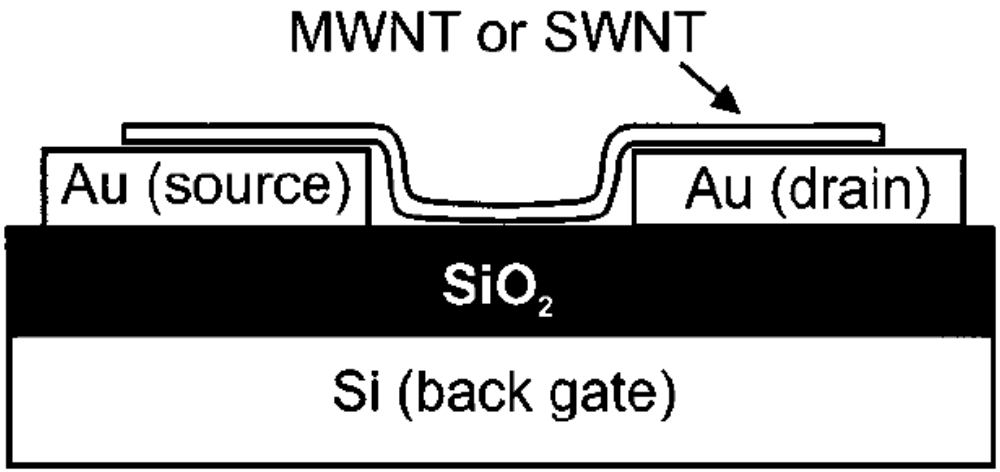

Figure 8. 10 A cross-section view of the nanotube FET device shows schematically a single carbon nanotube bridging the gap between two gold electrodes. The silicon substrate is used as back gate.

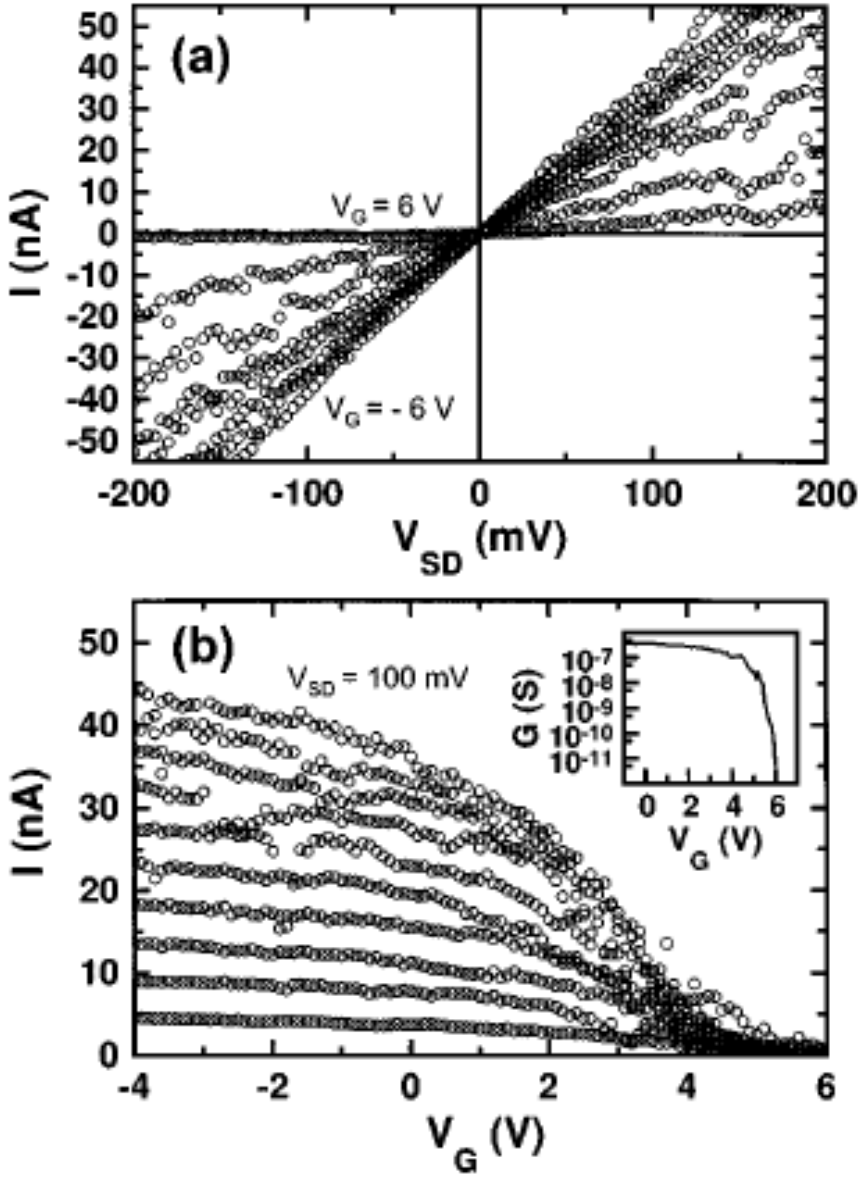

Figure 8. 11 Output and transfer characteristics for the SWNT FET schematically shown in Figure 10: (a) $I - V_{SD}$ curves measured for V_G= -6, 0, 1, 2, 3, 4, 5, and 6 V. (b) $I - V_G$ curves for V_{SD} = 10– 100 mV in steps of 10 mV. Inset shows that the gate modulates the conductance by 5 orders of magnitude (V_{SD} = 10 mV).

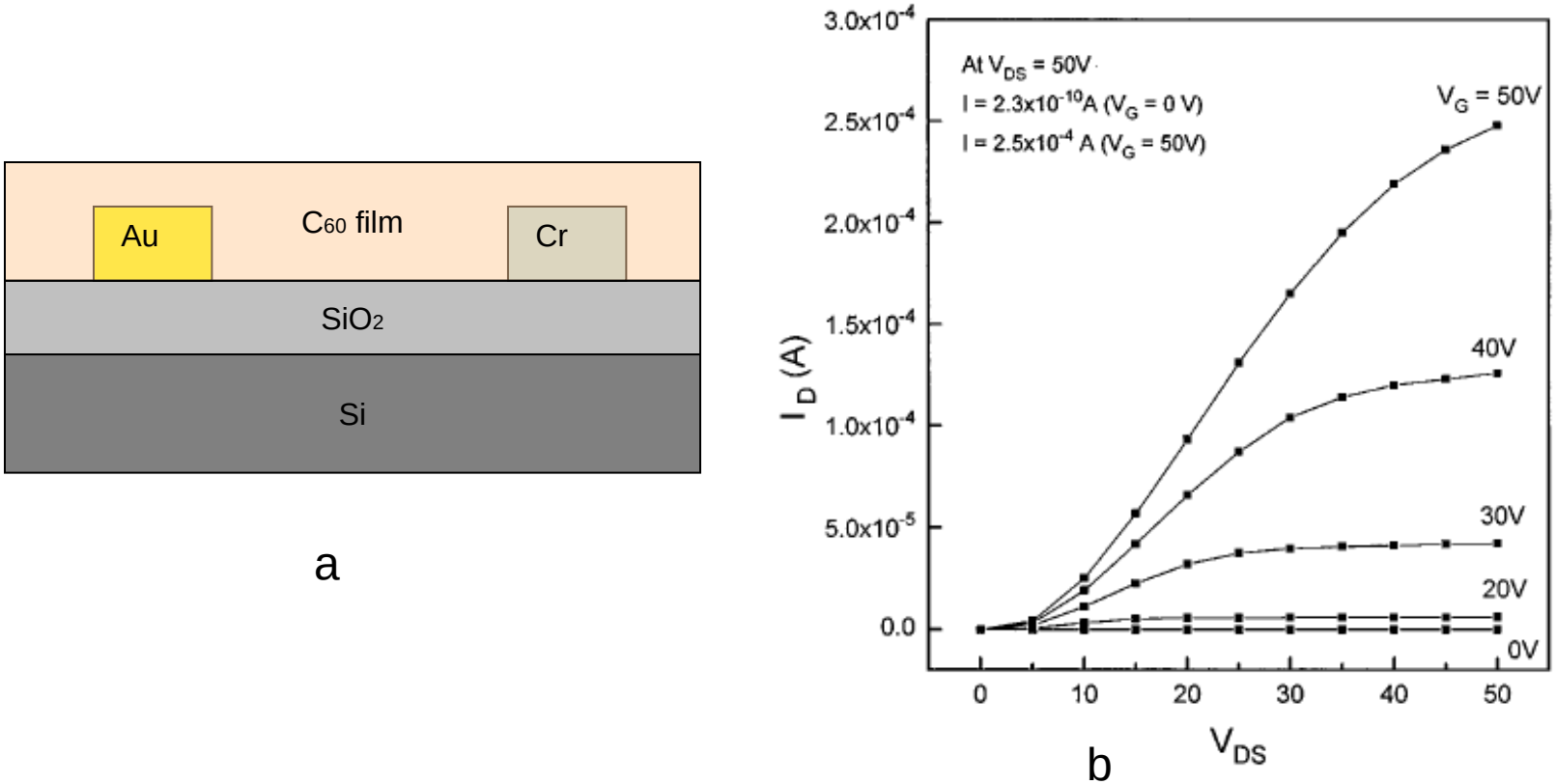

Figure 8. 12 (a) A schematic representation of the C_{60} thin film *n*-channel FET, and (b) drain current (I_D) *vs*. drain-source voltage (V_{DS}) under various gate voltages (V_G) for the C_{60} thin film transistor.

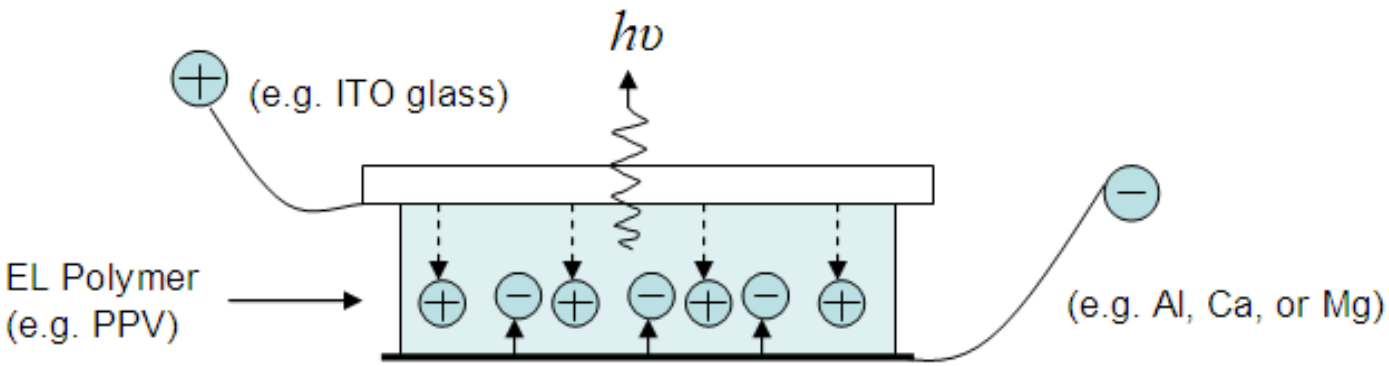

Figure 8. **13** Schematic representation of a single-layer polymer LED.

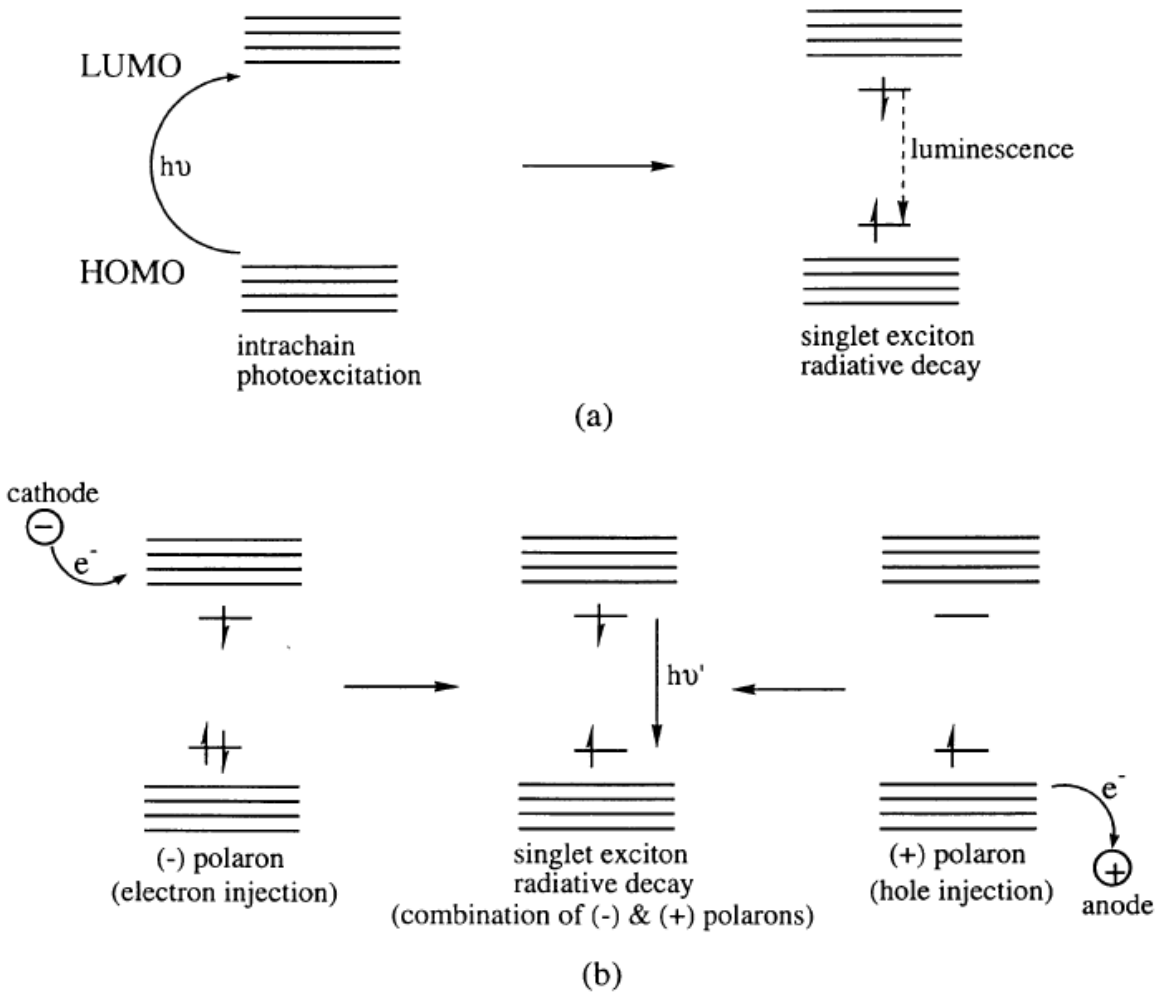

Figure 8. 14 The working principle for (a) PL and (b) EL.

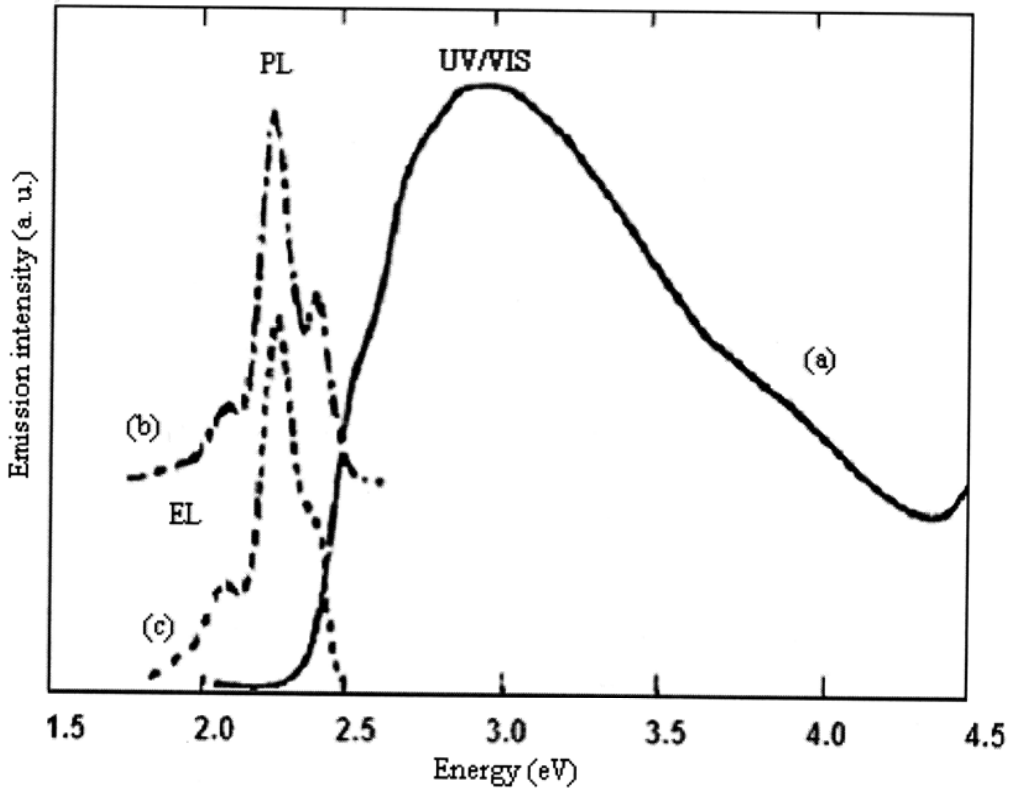

Figure 8. 15 The absorption (curve a) and emission (curves b and c) spectra of PPV. The similarity of the emission spectra generated by photoexcitation (Figure 14a) and by charge injection (Figure 14b) suggests that the same excited state is responsible for both photoluminescence (PL) and EL.

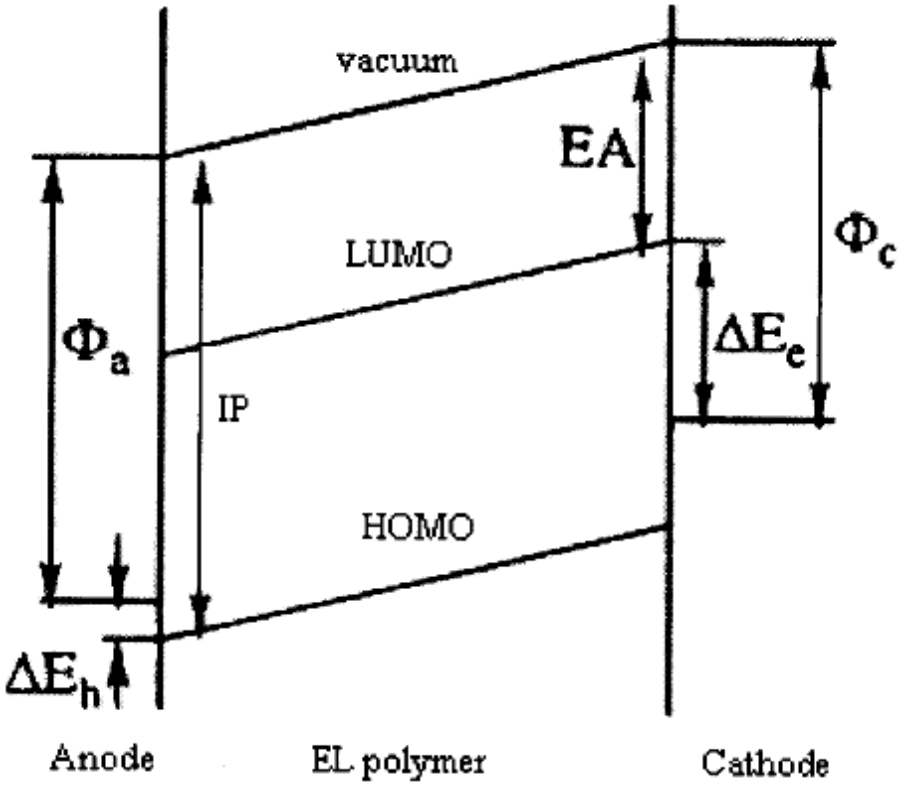

Figure 8. 16 A schematic energy level diagram.

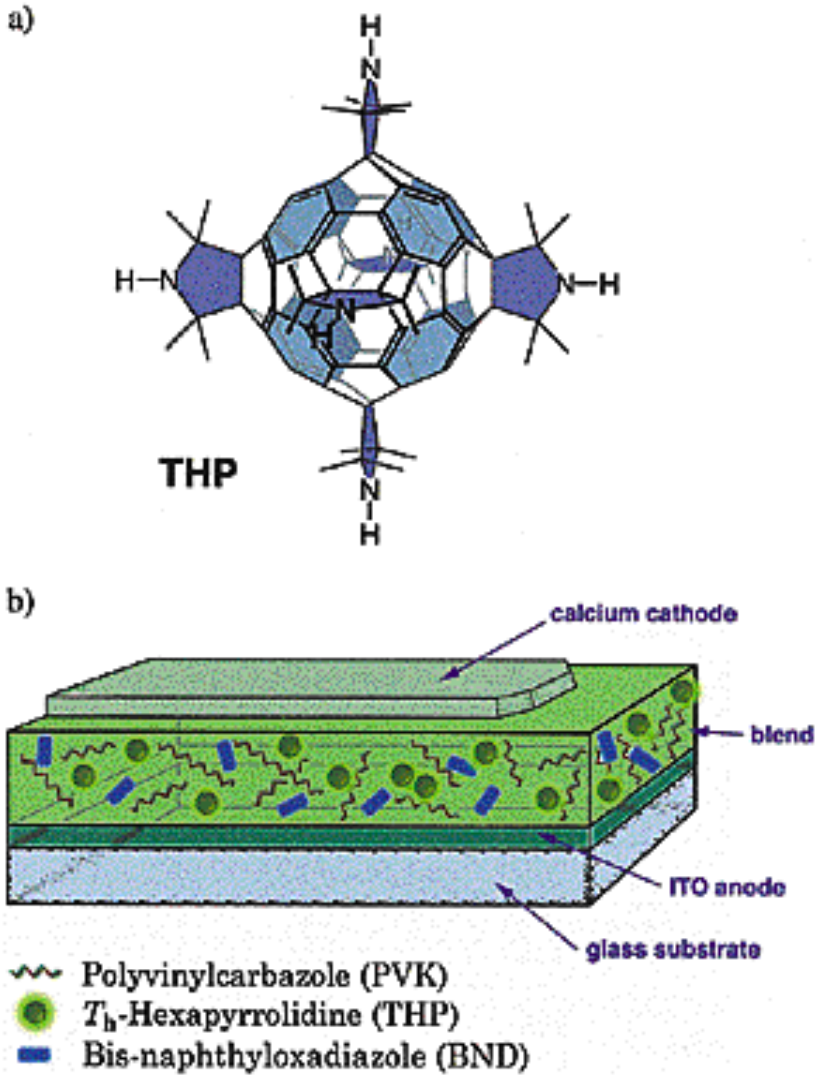

Figure 8. 17 (a) T_h-hexapyrrolidine (THP). (b) Device configuration.

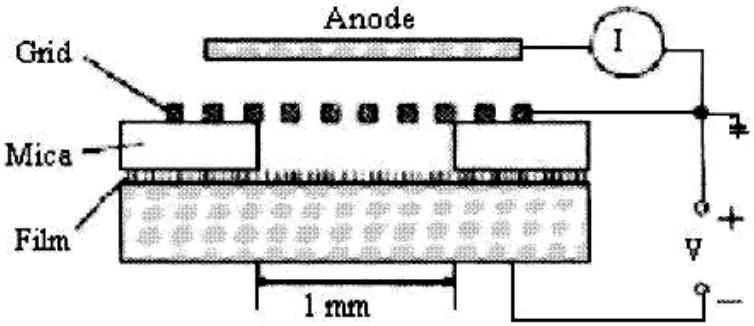

(a)

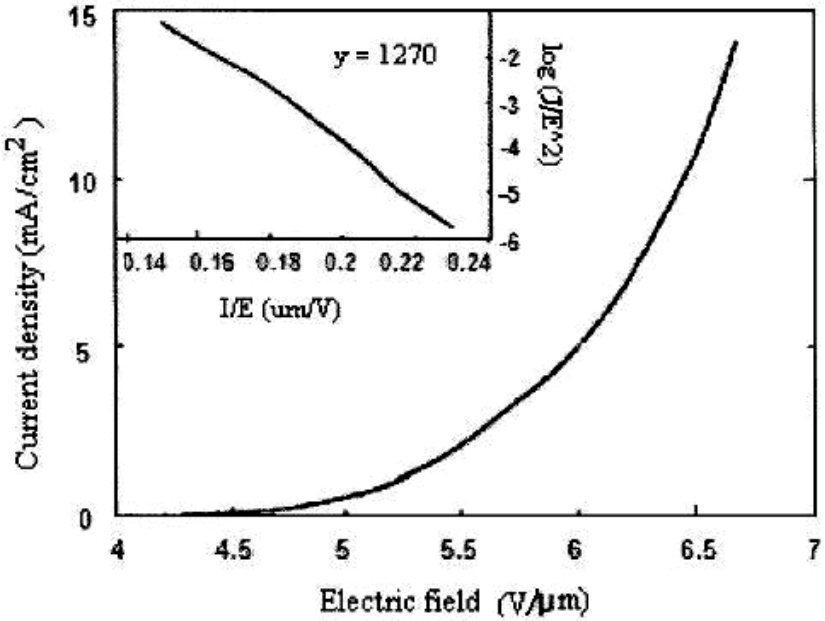

(b)

Figure 8. 18 (a) A schematic representation of a typical experimental set up for studying the field emission from aligned carbon nanotube films, and (b) the *I-V* curve for the aligned nanotube field emitter. Inset shows the Fowler-Nordheim plot of the emission current.

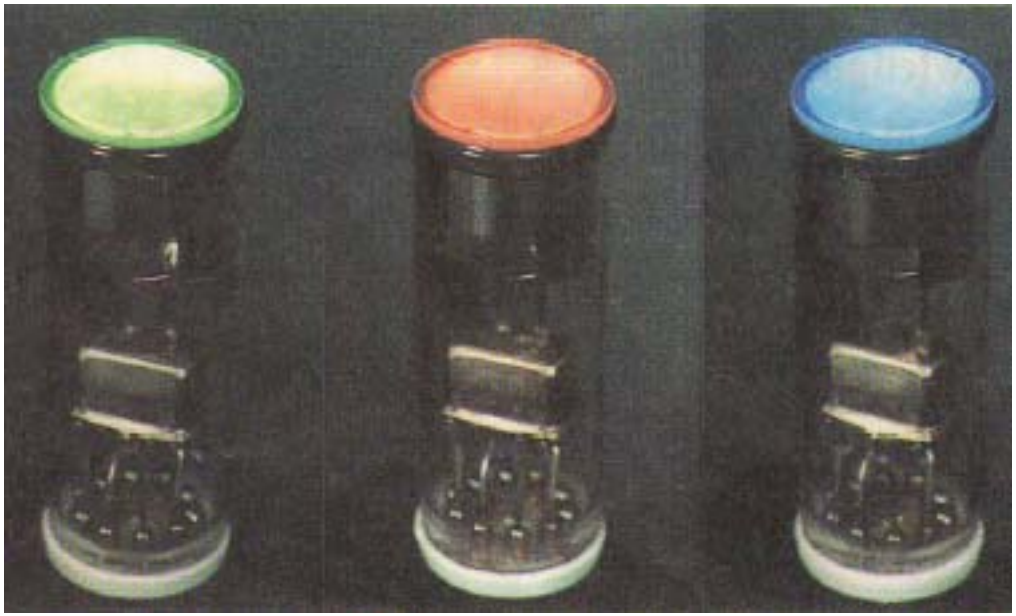

a

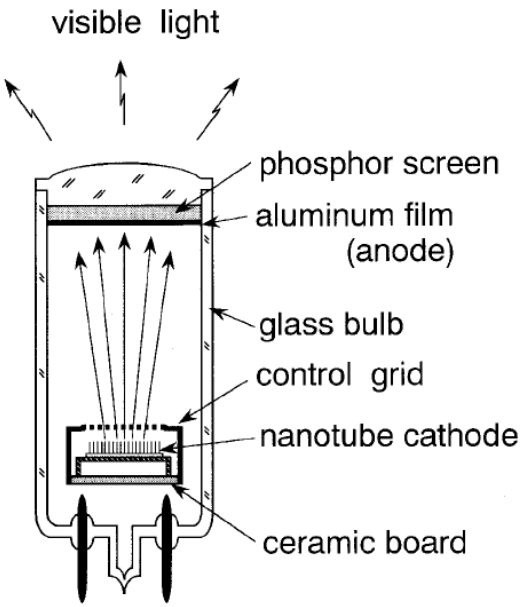

b

Figure 8. 19 (a) The cathode-ray lighting elements equipped with a carbon-nanotube field emitting cathode, displaying the three primary colors: green (ZnS:Cu, Al), red (Y_2O_3:Eu), and blue (ZnS:Ag); (b) a schematic presentation of the carbon nanotube field-emission lamps, in which electrons are extracted from the cathode by applying a voltage to the control grid. The electrons are accelerated towards the phosphor screen, which consequently emits light. The color of the light depends on the choice of the phosphor.

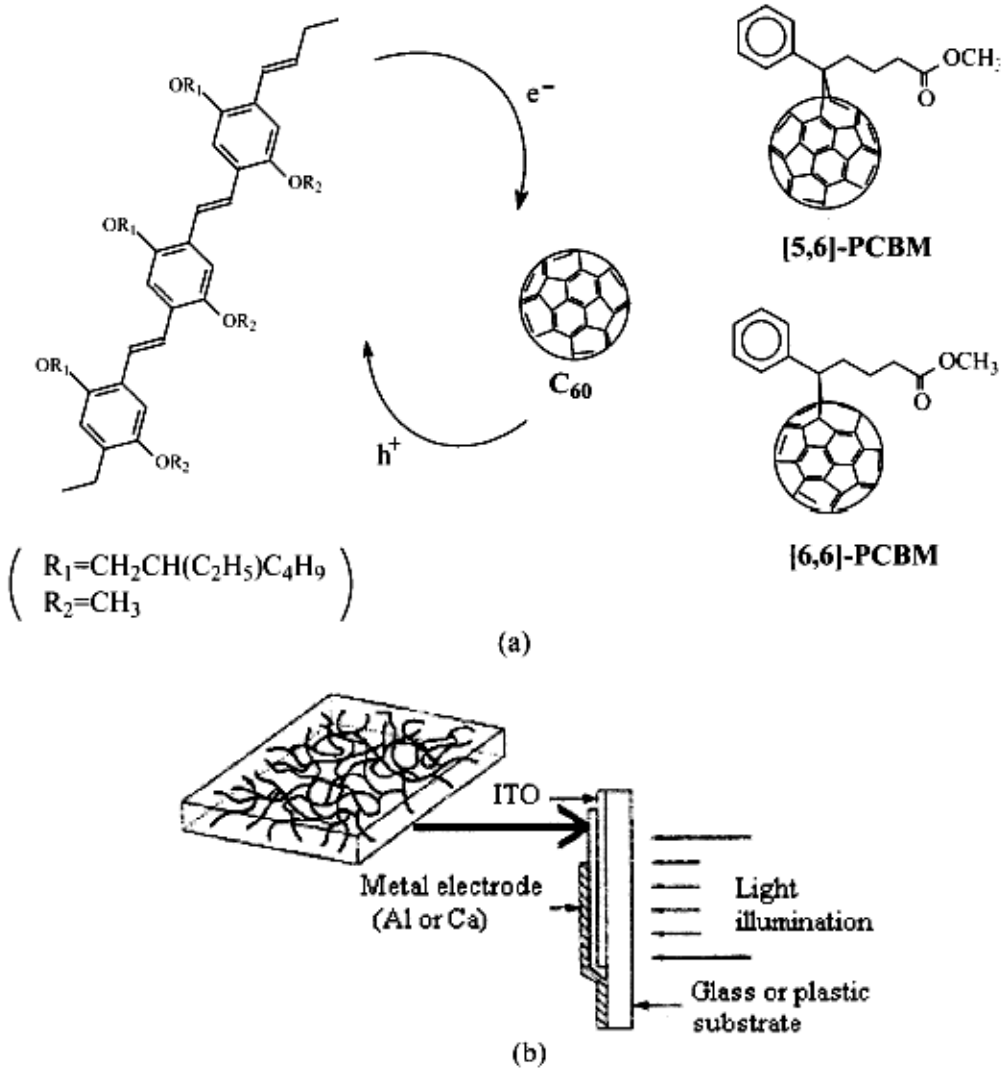

Figure 8. 20 Schematic illustrations (a) charge transfer between C_{60} derivatives and MEHPPV, and (b) the interpenetrating conjugated polymer-C_{60} (donor-acceptor) network and the photovoltaic cell.

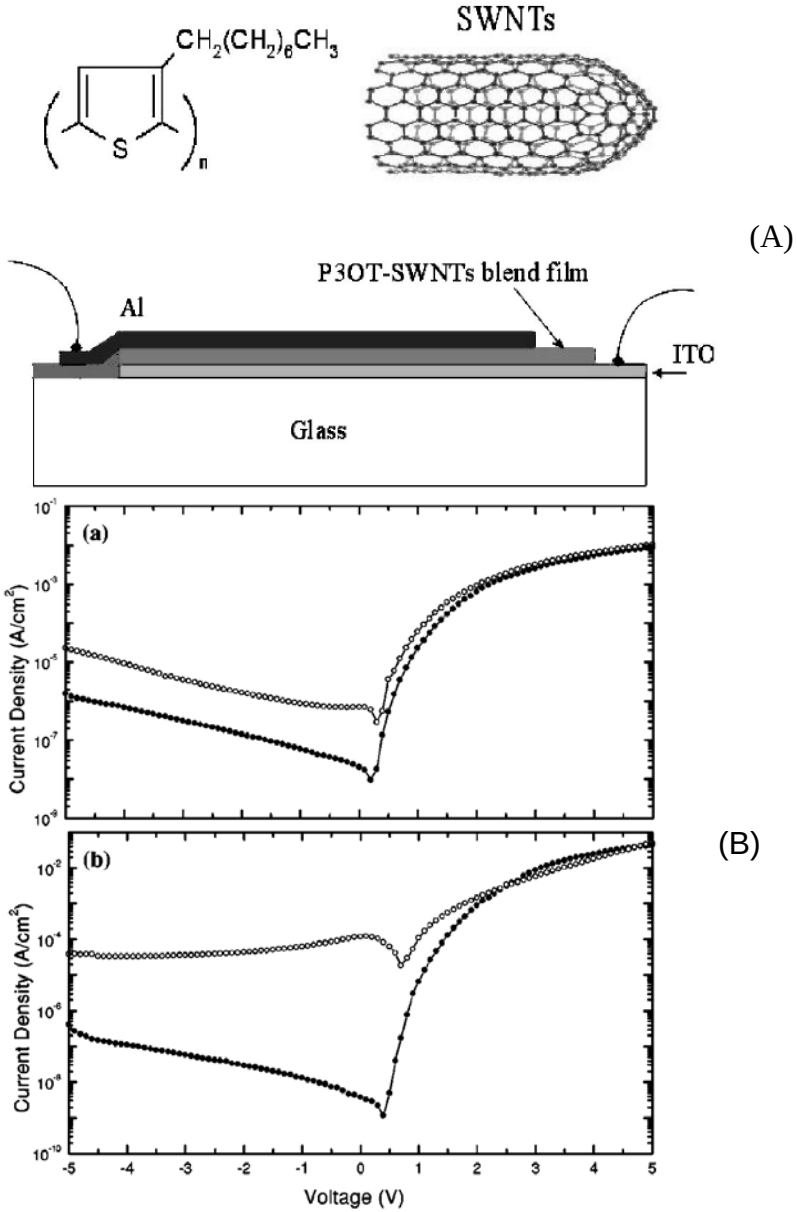

Figure 21. (A) A typical device architecture of the P3OT/SWNT photovoltaic ell. (B) (a) I-V characteristic of an ITO/P3OT/Al device in dark (filled circles) and under illumination (open circles); (b) the same data for an ITO/P3OT-SWNT/AI device.